

# High precision temperature- and energy-dependent refractive index of GaAs determined from excitation of optical waveguide eigenmodes

S. R. Kisting, P. W. Bohn, E. Andideh, I. Adesida, B. T. Cunningham, and G. E. Stillman

Department of Chemistry, Electrical Engineering Research Laboratory, Center for Compound Semiconductor Microelectronics, and Materials Research Laboratory, University of Illinois at Urbana-Champaign, 1209 West California Street, Urbana, Illinois 61801

T. D. Harris

AT&T Bell Laboratories, 600 Mountain Avenue, Murray Hill, New Jersey 07974

(Received 30 April 1990; accepted for publication 3 July 1990)

A GaAs-Al<sub>0.22</sub>Ga<sub>0.78</sub>As heterostructure was prepared and used as a multimode optical waveguide. Propagation constants for individual modes were measured by exciting one mode at a time via real-space surface grating couplers, and the resulting eigenmode distributions were used to obtain the refractive index of GaAs at a matrix of temperatures and photon energies spanning 40 K <  $T$  < 300 K and 1.40 eV <  $h\nu$  < 1.50 eV. Values for  $dn/dT$  and the extrapolated refractive index at  $T = 0$  K were also obtained. The dominant error source in these measurements was uncertainty in the angular placement of the sample. These measurements agree well with the few pre-existing temperature-dependent measurements, but are an order of magnitude more precise.

The optoelectronic properties of III-V semiconductors can be manipulated by adjusting impurity chemistry. The behavior of these materials depends on the type, extent, and spatial distribution of impurities incorporated in the lattice. To study impurity chemistry, probes are needed which are capable of chemical specificity, high sensitivity, and high spatial resolution. By combining waveguide-based optical depth profiling (ODP)<sup>1-3</sup> with low-temperature luminescence and inelastic scattering, all of these issues can be addressed. Extracting spatial information from the ODP experiment requires precise knowledge of the electric field amplitude distributions for each waveguide eigenmode. These distributions are intimately tied to the refractive indices of the superstrate, film, and substrate of the waveguide. Hence, full exploitation of the advantages of ODP requires accurate refractive index data over a wide range of temperatures and subband-gap photon energies. Here we present an accurate method for extracting the refractive index from any material which can be fabricated as a slab optical waveguide, and use the method to obtain new refractive index data for GaAs at a wide variety of temperatures and photon energies.

Several investigators have measured the dispersion of GaAs at energies surrounding the intrinsic band edge. Marple measured GaAs dispersion using prism refraction for three temperatures over a large range of subband-gap energies.<sup>4</sup> Sell *et al.* used a double beam reflection measurement on  $n$ - and  $p$ -type GaAs to determine refractive index values both above and below the intrinsic band gap.<sup>5</sup> Afromowitz has presented a semi-empirical method for determining the room-temperature index of refraction for Al <sub>$x$</sub> Ga<sub>1- $x$</sub> As.<sup>6</sup> In work presented here the subband-gap optical dispersion of semi-insulating GaAs has been mapped from 1.400 eV up to the start of the Urbach tail for temperatures 40–300 K through excitation of single eigenmodes in a GaAs/AlGaAs grating-coupled waveguide.

The use of the optical waveguide affords much higher precision than other techniques due to the high sensitivity of waveguide eigenmodes to the refractive index of the guiding layer.<sup>7,8</sup>

Consideration of the optical waveguide boundary value problem yields, for the waveguide eigenmodes,

$$kn_f t \cos \theta_f - \phi_s - \phi_c = m\pi, \quad (1)$$

where  $k$  is the wave vector of the incident light,  $n_f$  is the refractive index of the waveguide layer,  $t$  is the thickness of the guiding layer,  $\theta_f$  is the waveguide angle referenced to the surface normal,  $\phi_s$  and  $\phi_c$  are the substrate and cover interfacial phase shifts, and  $m$  is an integer which identifies the mode number.<sup>9</sup> Assuming known superstrate and substrate refractive indices, the film refractive index and thickness can be determined by measuring the propagation angles for at least two eigenmodes. Mode angles are measured by rotating the sample to allow exclusive excitation of each eigenmode during the angle scan. For at least two values of  $\theta_f$  and  $m$ , Eq. (1) can be solved by iterating values of  $n_f$  and  $t$  until the relation is satisfied. If three or more mode angles are recorded, an overdetermination of film parameters can be performed.<sup>10</sup>

Near-infrared laser radiation is coupled into the waveguide through diffraction gratings fabricated into the surface of the guiding layer at angles given by

$$n_f \sin \theta_f = n_1 \sin \theta_1 + \nu\lambda/L, \quad (2)$$

where  $n_1$  is the superstrate refractive index,  $\theta_1$  is the coupling angle with respect to the grating normal,  $\nu$  is the order of the diffraction,  $L$  is the grating periodicity, and  $\lambda$  is the wavelength of the incident light. An angle scan consists of recording eigenmode intensities as a function of  $\theta_1$ . Values of  $\theta_1$  can be converted to values of  $\theta_f$  through Eq. (2).

The waveguide sample consisted of a 2- $\mu\text{m}$ -thick epitaxial layer of high-purity GaAs grown over a 5  $\mu\text{m}$  layer of  $\text{Al}_{0.22}\text{Ga}_{0.78}\text{As}$  by metalorganic chemical vapor deposition (MOCVD) on semi-insulating bulk GaAs. A series of 200  $\mu\text{m} \times 200 \mu\text{m}$  diffraction gratings were written into a polymethylmethacrylate photoresist layer using electron beam lithography and then transferred to the epilayer using a reactive ion etch. The grating period was determined through a reflective diffraction experiment to be  $2496.0 \pm 0.2 \text{ \AA}$ . The cryostat is designed to allow sample rotation such that the input diffraction grating is over the center of rotation using a special  $360^\circ$  view optical dewar tail. This condition is necessary to ensure that the input grating does not translate relative to the input laser during the scan. Subband-gap near-infrared radiation was provided by an  $\text{Ar}^+$  pumped Ti:sapphire ring laser and focused with the appropriate polarization optics onto an input grating where the  $+1$  diffraction order was coupled into the various transverse electric (TE) eigenmodes. The entire waveguide was monitored by imaging the active layer with a charge-coupled device television (CCD TV) camera. Guided radiation was outcoupled at a grating further down the guide and detected by the camera. The image of the outcoupling grating was then transferred to a photomultiplier where Rayleigh scatter was detected using lock-in techniques. The entire process was controlled through the use of a laboratory personal computer.

Angle scans were carried out between 40 and 300 K in 20 K increments at photon energies from 1.400 eV up to the optical band edge. All scans yielded four to six TE eigenmodes. For photon energies within 30 meV of the band edge, absorption due to the Urbach tail became troublesome, manifesting itself by an obvious decrease in the intensity of guided radiation and an increased mode spacing. This often forced the loss of a mode when compared to scans at lower photon energy. These phenomena have also been noted by Swalen *et al.* for polymer waveguides.<sup>11</sup> The scans at nonabsorbing wavelengths ( $E_{\text{photon}} < E_{\text{gap}} - 30 \text{ meV}$ ) showed five or six TE modes and were fit to Eq. (1) to produce refractive index values. To determine the refractive index and thickness for the film, the fitting routine requires the angular values of the eigenmodes along with the mode number, and the superstrate and substrate refractive indices. The refractive index of the AlGaAs substrate is not known and is thus iterated until a minimum is found in the error sum. Hence at least three eigenmodes are required for this fit. A typical angle scan appears in Fig. 1, which shows eigenmode intensities versus coupling angle at 40 K and 1.490 eV. A fit of this data yields a refractive index of 3.604 and a film thickness of 2.04  $\mu\text{m}$ . Several angle scans were recorded at each photon energy-temperature pair, and the resulting TE eigenmode positions were averaged and used to produce refractive index values. The eigenmodes are sensitive to temperature changes as small as 4 K and photon energy changes on the order of 5 meV.

Table I lists the refractive indices determined for GaAs as a function of photon energy and temperature. GaAs

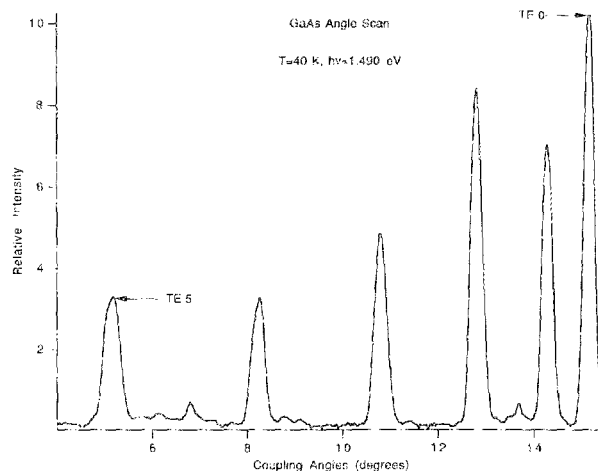


FIG. 1. Typical TE-polarized angle scan for the heterostructure at  $T = 40 \text{ K}$  and  $E = 1.490 \text{ eV}$ .

energy dispersion data can be fit to a first-order Sellmeier equation of the form

$$(n^2 - A) = n_\infty^2 - A / [1 - B(h\nu)^2] \quad (3)$$

constrained by three parameters  $A$ ,  $B$ , and  $n_\infty$ .<sup>12</sup> The dispersion data calculated at each temperature are consistent with Eq. (3), and a typical fit is shown in Fig. 2. The  $n_\infty$  parameter is the high-frequency dielectric constant. The refractive index of the AlGaAs was also fit along with the GaAs refractive index and GaAs thickness; however the recovered values for AlGaAs dispersion were not nearly as well behaved as those for GaAs. Because the percentage of the electric field amplitude distribution,

TABLE I. Temperature- and energy-dependent refractive index data for GaAs.

Temp. Energy (eV)	40 K	60 K	80 K	100 K	120 K	140 K
1.400	3.517	3.523	3.534	3.538	3.545	3.546
1.410	3.523	3.526	3.537	3.539	3.548	3.553
1.420	3.529	3.533	3.540	3.546	3.560	3.564
1.430	3.541	3.544	3.550	3.554	3.568	3.573
1.440	3.552	3.552	3.557	3.563	3.576	3.578
1.450	3.560	3.561	3.564	3.570	3.584	3.594
1.460	3.568	3.569	3.573	3.580	3.594	
1.470	3.578	3.578	3.584	3.592		
1.480	3.589	3.590	3.598			
1.490	3.604					
1.500	3.615					
Temp. Energy eV	160 K	180 K	200 K	220 K	240 K	
1.400	3.554	3.559	3.567	3.578	3.586	
1.410	3.559	3.569	3.578	3.589	3.600	
1.420	3.572	3.577	3.588	3.600		
1.430	3.582	3.587	3.608			
1.440	3.593					

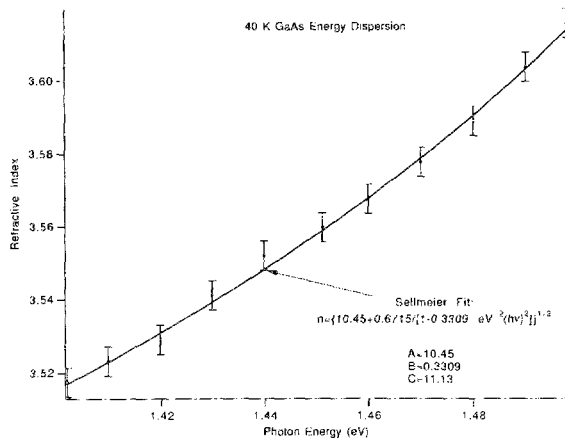


FIG. 2. Dispersion of the refractive index of GaAs at 40 K and the fit to the Sellmeier equation. Error bars were calculated from angular uncertainty and represent the estimated accuracy of the measurements.

which resides in the substrate material ranges between 0.2% for  $TE_0$  and 12% for  $TE_4$ , the AlGaAs does not carry a sufficiently large fraction of the total field to make our measurements sensitive to its refractive index.

The GaAs refractive index values can also be plotted at constant photon energy as a function of temperature in order to calculate a value for the temperature dispersion of GaAs. The refractive index of GaAs increases for a given photon energy as the temperature increases. A linear fit of this data yields the temperature dispersion constant,  $(dn/dT)$ , and  $n(T=0)$ , the refractive index extrapolated to 0 K. Values for the temperature dispersion and 0 K refractive index at various subband-gap energies are listed in Table II. Angle scan fits provide values for both the refractive index and the thickness of the guiding layer. From values of the coefficient of linear expansion, it is estimated that the film thickness will change approximately 0.1% over the range of temperatures used in this work, which is negligible when compared to the precision of the thickness measurement, which is  $\sim 1\%$ . Over the 68 fits performed the average of the best-fit thicknesses was calculated to be

TABLE II. Temperature parameters for linear fits.

Photon energy (eV)	$n(T=0 \text{ K})$	$dn/dT$ ( $\times 10^{-4}$ )
1.400	3.504	3.224
1.410	3.504	3.763
1.420	3.510	3.924
1.430	3.519	4.047
1.440	3.533	3.411
1.450	3.540	3.558
1.460	3.551	3.230

$2.05 \pm 0.02 \mu\text{m}$ , in good agreement with the targeted thickness of  $2 \mu\text{m}$  for the MOCVD process.

The major source of error in the calculation of the refractive index data is in the angular values of the eigenmodes. The value of the coupling angle was initially set at  $0^\circ$  by rotating the sample until the backreflection off the input grating propagated through an entrance aperture in the optical train. The width of this aperture introduced an error of  $\pm 0.02^\circ$  in the value of the coupling angle. Another source of error in this angle is in the movement of the rotational stage. Independent experiments showed it to be accurate within  $\pm 0.1^\circ$ . All other variables in Eq. (2) are assumed to have a negligible error when compared to the coupling angle. Numerical evaluations of the accuracy of the best-fit refractive index values yielded a maximum change in the best-fit refractive index of  $\pm 0.004$ . This value should be a reasonable estimate for the accuracy of the refractive index values shown in Table I. It should be noted that this value for the accuracy is much higher than the typical  $\pm 0.0005$  precision obtained from the fit of the propagation constant data to Eq. (1).

In summary, the refractive index of semi-insulating GaAs has been determined as a function of both temperature and subband-gap photon energy by direct observation of eigenmode propagation constants in grating coupled slab waveguides. The advantage of this technique is that the propagation constants are a very sensitive indicator of refractive index changes in the waveguide. This provides an excellent way to detect small changes in the refractive index due to changes in temperature and photon energy. Results for the energy and temperature dispersion of GaAs are consistent with, but extend existing models.

This work was supported by the National Science Foundation grants DMR 8920538, DRM 8920538, and CHE 8800992, and by a National Nanofabrication Facility facilities use grant. The authors wish to thank T. DeTemple for the loan of an infrared CCD TV camera for early portions of this work.

<sup>1</sup>P. W. Bohn, *Anal. Chem.* **57**, 1203 (1985).

<sup>2</sup>D. R. Miller, O. H. Han, and P. W. Bohn, *Appl. Spectrosc.* **41**, 245 (1987).

<sup>3</sup>D. R. Miller, O. H. Han, and P. W. Bohn, *Appl. Spectrosc.* **41**, 249 (1987).

<sup>4</sup>D. T. F. Marple, *J. Appl. Phys.* **35**, 1241 (1964).

<sup>5</sup>D. D. Sell, H. C. Casey, Jr., and K. W. Wecht, *J. Appl. Phys.* **45**, 2650 (1974).

<sup>6</sup>M. A. Afromowitz, *Solid State Commun.* **15**, 59 (1974).

<sup>7</sup>S. Morasca, B. Sordo, C. DeBenardi, and M. Meliga, *Appl. Phys. Lett.* **52**, 1593 (1988).

<sup>8</sup>M. Meliga, S. Morasca, B. Sordo, and C. DeBenardi, *Proc. Soc. Photo-Opt. Instrum. Engr.* **835**, 251 (1987).

<sup>9</sup>D. Marcuse, *Theory of Dielectric Optical Waveguides* (Academic, New York, 1974), Chap. 1.

<sup>10</sup>R. Ulrich and R. Torge, *Appl. Opt.* **12**, 2901 (1973).

<sup>11</sup>J. D. Swalen, M. Tacke, R. Santo, K. E. Rieckhoff, and J. Fischer, *Helv. Chim. Acta* **61**, 960 (1978).

<sup>12</sup>J. S. Blakemore, *J. Appl. Phys.* **53**, R123 (1982).